Molecular hydrogen accelerates the reversal of acute obstructive cholangitis-induced liver dysfunction by restoring gap and tight junctions

ZHIYANG ZHU[1*], JIANHUA YU[1*], WEIGUO LIN[1], HAIJUN TANG[1], WEIGUANG ZHANG[2] and BAOCHUN LU[1]

[1]Department of Hepatobiliary Surgery, Shaoxing People's Hospital (Shaoxing Hospital, Zhejiang University School of Medicine); [2]Department of Molecular Medicine and Clinical Laboratory, Shaoxing Second Hospital, Shaoxing, Zhejiang 312000, P.R. China

Received October 1, 2018; Accepted March 27, 2019

DOI: 10.3892/mmr.2019.10179

Abstract. Gap junctions (GJs) and tight junctions (TJs) are essential to maintain the function of hepatocytes. Changes in biliary tract pressure and the effect of lipopolysaccharide (LPS) may lead to acute obstructive cholangitis (AOC) and cause liver injury via GJ and TJ dysfunction. Hydrogen has been confirmed to have a protective role in various organs during pathological conditions and inflammation. The present study investigated the function of junction proteins and the potential application of H_2 in AOC-induced liver injury. An AOC rat model was established by LPS injection through a bile duct catheter, while the distal bile duct was closed. The catheter sealing caps were removed and bile was allowed to flow out from the catheters at 12 h after LPS infusion. The potential application of H_2 was studied in the AOC rat model with biliary drainage. It was observed that AOC induced the disruption of junction proteins of both GJs and TJs. H_2 administration reversed AOC-induced disruption of GJs and TJs after biliary drainage. The mechanism of this phenomenon suggests that H_2 may have effectively attenuated AOC-induced inflammatory and oxidative damage, and decreased matrix metalloproteinase activity. H_2 may accelerate the reversal of AOC-induced liver dysfunction, and this phenomenon may depend on reversing the inhibition of GJs and TJs.

Introduction

The function of the 'blood-biliary barrier' is to ensure bile secretion without leakage from the centrizonal region to the periportal zone and then to bile ducts, in a highly ordered manner (1). Because gap junctions (GJs) regulate direct intercellular communication and tight junctions (TJs) completely seal the bile canaliculi, these are essential to maintain the function of the blood-biliary barrier (1). The most common GJ proteins in the liver, the connexins (Cx, also termed gap junction proteins) Cx26 (gap junction protein β2) and Cx32 (gap junction protein β1) have been found to be downregulated during obstructive cholestasis and lipopolysaccharide (LPS)-induced hepatocellular cholestasis (2). In addition, expression of TJ proteins, such as tight junction protein 1 (ZO1/TJP1), has also been reported to be influenced by LPS or liver injury (3,4). Alterations in GJ and TJ composition are associated with hepatic disease and lead to cholangiovenous reflux, liver injury, and even systemic disease (1). Acute obstructive cholangitis (AOC) is a bacterial infection caused by biliary obstruction, and it leads to systemic signs of infection (5). Due to the high biliary pressure and the presence of LPS, blood-biliary barrier disruption may occur in cases of AOC (5). In severe cases of AOC, LPS and cholochrome may be continuously released into the blood until functional restoration of the barrier occurs (5). Therefore, accelerating the restoration of hepatocyte GJs and TJs may improve patient prognosis and shorten the course of AOC.

Molecular hydrogen (H_2) is regarded as an important physiological regulatory factor with antioxidant effects, which protect cells and organs from injury caused by reactive oxygen species (ROS) and oxidative stress (6-8). Anti-inflammatory effects are another important physiological regulatory function of H_2 (6). H_2 may therefore be a promising therapeutic strategy to combat certain pathologies and sepsis (9-11). Given that H_2 serves important physiological functions, it is possible that H_2 may have a role in the process of AOC.

Therefore, the present study hypothesized that H_2 administration may help reverse the AOC-induced disruption of GJs and TJs in hepatocytes and accelerate the tissue recovery process.

Materials and methods

Experimental animals. Male Wistar rats, weighing 300-350 g (13-16 weeks old) were purchased from Shanghai SLAC

Correspondence to: Dr Baochun Lu, Department of Hepatobiliary Surgery, Shaoxing People's Hospital (Shaoxing Hospital, Zhejiang University School of Medicine), 568 North Zhongxing Road, Shaoxing, Zhejiang 312000, P.R. China
E-mail: sygd_lbc@126.com

[*]Contributed equally

Key words: acute obstructive cholangitis, molecular hydrogen, blood-biliary barrier, gap junctions, tight junctions

Laboratory Animal Co., Ltd. All procedures were approved by the Ethics Committee of Zhejiang University, and conformed to the Care and Use of Laboratory Animals Guide published by the US National Institutes of Health (NIH Publication no. 85e23, revised 1996). The rats had *ad libitum* access to food and water, and were maintained at 20˚C, with 50% humidity under 12:12-h light-dark cycles.

Establishment of rat AOC models. A total of 19 rats were randomly assigned to the following three groups (n≥6 rats/group): Sham; bile duct ligation (BDL); and acute obstructive cholangitis (AOC) groups. Intraperitoneal injections of pentobarbital (50 mg/kg) were used to anaesthetize the animals. In the BDL and AOC groups, the distal common bile ducts were dissociated and ligated with 6-0 silk sutures. PE-10 polyethylene catheters (~3 cm), which were long enough to reach the skin surface of the animals, were inserted into the proximal bile ducts as previously described (12). Intra-bile duct infusions were performed immediately following surgery. For intra-bile duct infusions, 0.2 ml of saline or LPS (2 mg/ml, purified from *Escherichia coli* O111:B4; Sigma-Aldrich, Merck KGaA) was injected into the proximal bile ducts through the catheters. After injection of 0.1 ml air, the catheter was sealed with a sealing cap and the abdominal cavity was closed using silk sutures. Rats in the sham group underwent a sham operation.

According to the specific symptoms associated with this model and the guidelines suggested by previous studies (13,14), humane endpoints were defined as lethargy (lack of response to stimulus), hypopnea, cyanosis or hypothermia at 34˚C. Animals that exhibited any of these symptoms were sacrificed via cervical dislocation under isoflurane anesthesia. After a 12-h observation period, during which 1 rat was sacrificed after reaching the aforementioned humane endpoints, the remaining 18 rats were sacrificed, and blood and tissue samples were harvested. Blood samples were centrifuged (1,000 x g for 5 min at 4˚C) and serum was stored at -80˚C prior to subsequent analysis. Liver fractions were snap-frozen in liquid nitrogen and then stored at -80˚C.

Preparation of hydrogen-rich saline (HRS). HRS was prepared as previously described (15,16). In brief, HRS was prepared by dissolving hydrogen in physiological saline for 12 h under high pressure (0.4 MPa). HRS was stored under atmospheric pressure at 4˚C in a sealed bag with no dead volume. Using gas chromatography according to a previously described protocol (17), the hydrogen concentration on the first day after preparation was 0.76±0.05 and 0.62±0.04 mmol/l at 7 days post-preparation. HRS was prepared weekly to ensure that the concentration of hydrogen was sufficient for experiments.

HRS administration experiment. A total of 30 AOC rats were divided into three groups in this part of experiment (n=10). The catheter sealing caps were removed and bile was allowed to flow out from the catheters at 12 h after LPS infusion. Normal saline (NS, 5 ml/kg) or HRS (5 and 10 ml/kg) was administered intraperitoneally from the day of surgery (once daily) until the end of the experiment (72 h following LPS infusion). All rats remained under strict observation (every 6 h) and time of death was recorded over a 72 h observation period after LPS infusion. During this observation period, animals that reached the aforementioned humane endpoints were sacrificed humanely under anesthesia. All other animals were sacrificed after the 72 h observation period, and blood and tissue samples were harvested from these animals only.

Evaluation of liver function. The serum levels of aspartate aminotransferase (AST), alanine aminotransferase (ALT) and total bilirubin (TBIL) were measured using an Automated Chemical Analyzer (Dimension RxLMax HM; Siemens AG) to evaluate the degree of liver injury and function.

Cell experiments. The rat hepatic cell line BRL was obtained from the Chinese Academy of Sciences Shanghai Branch Cell Bank. BRL cells were cultured in DMEM (Gibco, Thermo Fisher Scientific. Inc.) supplemented with 10% FBS (Gibco; Thermo Fisher Scientific, Inc.), 100 IU/ml penicillin and 100 μg/ml streptomycin, at 37˚C in an atmosphere with 5% CO_2.

The BRL cells ($1x10^6$) were seeded into 60 mm dishes. After 24 h of culture to allow cells to attach, cells were treated with or without LPS, at 400 ng/ml for 6 h. Cells were harvested and total proteins were extracted for western blot analysis.

Similar to the aforementioned method, BRL cells were treated with or without H_2O_2, at 200 μmol/l for 6 h. Cells were harvested and total proteins were extracted for western blot analysis.

RNA extraction and reverse transcription-quantitative PCR (RT-qPCR). Total RNA was isolated from liver tissue samples using TRIzol® (Invitrogen; Thermo Fisher Scientific, Inc.) and reverse transcribed into cDNA using the High-Capacity cDNA Reverse Transcription kit (Applied Biosystems; Thermo Fisher Scientific, Inc.), according to the manufacturer's instructions. Briefly, RT was conducted at 25˚C for 10 min, 37˚C for 120 min and 85˚C for 5 min; cDNA was stored at 4˚C until further use. The RT-qPCR was performed using SYBR®-Green PCR Master Mix and the ABI 7500 Real-time PCR system (both Applied Biosystems; Thermo Fisher Scientific, Inc.). Primers sequences used are provided in Table I. β-actin was used as an endogenous control. The RT-qPCR was performed according to the manufacturer's instructions. Briefly, the PCR conditions included 95˚C for 5 min, and a total of 40 cycles of 95˚C, 60˚C and 72˚C for 30 sec, followed by a final extension at 72˚C for 5 min. All assays were performed three times. Relative expression levels were then determined using the $2^{-\Delta\Delta Cq}$ method (18).

Western blot analysis. Total proteins were extracted from tissue samples or cells using lysis buffer containing phenylmethyl sulfonylfluoride (both from Beyotime Institute of Biotechnology) at 25˚C, and the protein concentration was determined using a BCA Protein Assay kit (Beyotime Institute of Biotechnology). On a 10% SDS-PAGE gel, 20 μg total protein was electrophoresed, transferred onto to polyvinylidene fluoride membranes, blocked with 5% non-fat milk for 1 h at room temperature, and incubated with the following primary antibodies: Anti-ZO1 (1:250; cat. no. ab59720; Abcam); anti-occludin, (1:500; cat. no. 13409-1-AP; ProteinTech Group,

Table I. Primer sequences.

Name	Symbol	Forward (5'-3')	Reverse (5'-3')
β-actin	ACTB	ACACCCGCCACCAGTTCG	CCCACGATGGAGGGGAAGA
ZO1	TJP1	TCGGAGCTCGGGCATTATTC	CAGGGCACCATACCAACCAT
Occludin	OCLN	CCCTTCTTTCCTTAGGCGACC	TGGGTTTGAATTCATCCGGC
Cx26	GJB2	CCACTTCTGACCAACCCAGG	CTCTGGATGGTTGGCACTGT
Cx32	GJB1	GACACGCCTGCATACATTCC	TCCTGCCTCATTCACACCTCC
Cx43	GJA1	TGAAAGAGAGGTGCCCAGACA	CACCCCAAGCTGACTCAACA
IL-6	IL6	TCTGCCCTTCAGGAACAGCTAT	TGTCAACAACATCAGTCCCAAGA
TNF-α	TNF	ACAGCAACTCCAGAACACCC	GGAGGGAGATGTGTTGCCTC
IL-1β	IL1β	GCTTCCTTGTGCAAGTGTCTG	AGTCAAGGGCTTGGAAGCAA

ZO1, tight junction protein 1; Cx26, gap junction protein β2; Cx32, gap junction protein β1; Cx43, gap junction protein α1; IL, interleukin; TNF-α, tumor necrosis factor-α.

Inc.); anti-Cx26 (1:500; cat. no. 16960-1-AP; ProteinTech Group, Inc.); anti-Cx43 (gap junction protein α1; 1:1,000; cat. no. 3512; Cell Signaling Technology, Inc.); anti-Cx32 (1:250; cat. no. sc-59948, Santa Cruz Biotechnology, Inc.); and anti-β-actin (1:1,000; cat. no. sc-4778; Santa Cruz Biotechnology, Inc.). All primary antibody incubations were performed overnight at 4˚C. The membranes were subsequently incubated with horseradish peroxidase-conjugated secondary antibodies (1:8,000; cat. nos. A0216 and A0208; Beyotime Institute of Biotechnology) for 2 h at room temperature. Immunoreactive bands were visualized using enhanced chemiluminescence reagent (Beyotime Institute of Biotechnology). β-actin was employed as an endogenous control. Quantity One 4.6.8 (Bio-Rad Laboratories, Inc.) was used for the quantification of expression.

Immunohistochemical staining. Liver tissue samples were fixed with 10% neutral formalin at room temperature overnight. ZO1 expression was detected immunohistochemically by sectioning (3-μm thickness) paraffin-embedded specimens from the different groups. After deparaffinization and rehydration of the sections, endogenous peroxidase activity was blocked using 0.3% hydrogen peroxide. The sections were blocked with 1% bovine serum albumin (Beyotime Institute of Biotechnology) for 2 h at room temperature. The sections were incubated with primary anti-ZO1 antibody (1:100; cat. no. ab59720; Abcam) overnight at 4˚C, followed by incubation with appropriate horseradish peroxidase-conjugated secondary antibodies (1:4,000; cat. no. A0208; Beyotime Institute of Biotechnology) for 1.5 h at room temperature. After a thorough washing, the sections were developed using a 3,3'-diaminobenzidine kit (cat. no. P0202; Beyotime Institute of Biotechnology) and counterstained with hematoxylin staining solution for 10 min at room temperature (cat. no. C0107; Beyotime Institute of Biotechnology). Each stained sample was observed using a light microscope (x200; Leica Microsystems, Inc.).

Measurement of superoxide dismutase (SOD) and malondialdehyde (MDA). Samples were homogenized and sonicated (25˚C, ~20-25 kHz, 2 sec) in cold saline to generate 5% homogenates. Aliquots of supernatants were prepared by centrifugation (4˚C, 12,000 x g, 5 min) and used for subsequent experiments. The supernatant was assayed for protein concentration using an enhanced bicinchoninic acid protein assay kit (Beyotime Institute of Biotechnology). Both measurements of SOD activity and MDA content in tissue homogenates were performed in accordance with the manufacturer's instructions (cat. nos. A001-3-1 and A003-1-1, respectively; Nanjing Jiancheng Bio-Engineering Institute Co., Ltd.). All assays were performed three times.

Gelatin gel zymography. Gelatin gel zymography was performed using a gelatin zymography assay kit (Shanghai Genmed Pharmaceutical Technology Co., Ltd.). Briefly, gels with gelatin were prepared in accordance with the manufacturer's instructions. After electrophoresis, gels were treated with a renaturation buffer, a digestive buffer, a staining buffer, an eluent buffer and a stop buffer, all supplied with the assay kit. The clear bands on the blue background reflected the proteolytic activity of matrix metalloproteinase (MMP)-2 and MMP-9.

Statistical analysis. Data are presented as the mean ± standard deviation. All assays were performed at least three times. Statistical significance between two groups was determined using the Student's t-test. One-way analysis of variance followed by Tukey-Kramer post-hoc tests were performed to examine differences among multiple groups. $P<0.05$ was considered to indicate a statistically significant difference. All statistical analyses were conducted using SPSS 13.0 (SPSS, Inc., Chicago, IL, USA).

Results

AOC induces disruption of hepatocyte GJs and TJs. Firstly, hepatic tests were used to verify liver function in the AOC animal model. ALT, AST and TBIL levels increased rapidly after BDL compared with those in the sham operation group, and these were further significantly increased in the AOC group (data not shown), which is similar to a previous study (19) and the classical changes observed in patients with AOC (Table II).

Table II. Liver function test results of the different rat models.

	Sham	BDL	AOC
ALT, IU/l	57.50±7.46	518.83±71.86[a]	848.67±67.74[a,b]
AST, IU/l	77.67±8.30	798.83±72.78[a]	1321.67±121.28[a,b]
TBIL, μmol/l	10.02±1.65	46.72±12.88[a]	68.93±10.21[a,b]

[a]P<0.05 vs. sham group; [b]P<0.05 vs. BDL group. ALT, alanine aminotransferase; AST, aspartate aminotransferase; TBIL, total bilirubin; BDL, bile duct ligation; AOC, acute obstructive cholangitis.

Secondly, GJ and TJ mRNA and protein expression in liver tissues were examined. RT-qPCR revealed that TJ protein mRNA expression in the AOC group, including ZO1 and occludin, decreased significantly compared with the BDL and sham groups (Fig. 1A). GJ protein expression, including Cx26 and Cx32, was also downregulated in the AOC group. Cx43 expression, another important GJ protein, was upregulated significantly in the AOC group compared with the other groups (Fig. 1A). Western blot analysis also confirmed that ZO1, occludin, Cx26 and Cx32 expression was downregulated in the AOC group (Fig. 1B and C). However, Cx43 protein levels did not change, which was unexpected (Fig. 1B and C). These results indicated that AOC induces aberrant TJ and GJ mRNA and protein expression.

Inflammatory and oxidative damage induces disruption of junction proteins in hepatocytes. Inflammatory and oxidative damage occurs across a variety of liver injuries (20,21). Therefore, the role of inflammatory and oxidative damage in AOC-induced liver injury was also evaluated in the present study. The results showed that the mRNA levels of inflammatory cytokines, including interleukin (IL)-6, tumor necrosis factor-α (TNF-α) and IL-1β, were upregulated significantly in the AOC group compared with the other groups (Fig. 2A). Hepatic SOD and MDA were also measured to evaluate oxidative damage during AOC. Compared with the BDL group, the AOC group had higher levels of MDA and lower levels of SOD activity (Fig. 2B and C).

In vitro cell experiments were performed to further elucidate the association between the disruption of junction proteins and inflammatory or oxidative damage. This was performed by examining TJ and GJ protein expression levels in cultured BRL cells after LPS or H_2O_2 treatment, respectively. The results showed that the expression of ZO1, occludin, Cx26 and Cx32 was significantly downregulated following treatment with LPS, while Cx43 expression was upregulated (Fig. 2D). Following exposure to H_2O_2, Cx32 expression did not change significantly, while ZO1, occludin, Cx26 and Cx43 expression levels were significantly decreased (Fig. 2E). The cell experiments showed that both inflammatory damage and oxidative damage induced aberrant TJ and GJ protein expression. Notably, these changes were similar to those observed in the livers of AOC rats. These results indicated that aberrant TJ and GJ protein expression during AOC may be attributed to inflammatory and oxidative damage.

Molecular hydrogen attenuates AOC-induced inflammatory and oxidative damage. H_2 has been reported to exhibit antioxidant and anti-inflammatory properties (6). Thus, the potential protective role of H_2 against inflammatory and oxidative liver damage induced by AOC was further assessed. IL-6, TNF-α and IL-1β were analyzed to evaluate the levels of inflammation with or without HRS administration. The results showed that HRS administration significantly mitigated the increase in inflammatory cytokine expression (Fig. 3A). Compared with the NS group, SOD activity was increased in the liver tissues after administration of HRS (Fig. 3B). Conversely, treatment with HRS significantly lowered the levels of MDA (Fig. 3C). These results indicated that H_2 may have attenuated the AOC-induced inflammatory and oxidative damage.

H_2 reverses AOC-induced disruption of junction proteins and decreases the activity of MMPs. To clarify the relationship between the function of H_2 and the blood-biliary barrier, GJ and TJ mRNA expression were evaluated after biliary drainage and HRS administration. The results showed that occludin, Cx26 and Cx32 mRNA expression were upregulated significantly after treatment with HRS compared with rats that received NS (Fig. 4A). The other junction proteins, ZO1 and Cx43, were not affected by either treatment (Fig. 4A). However, the western blotting results indicated that all GJ and TJ proteins, including ZO1 and Cx43, were upregulated significantly following HRS administration (Fig. 4B and C). Immunohistochemistry also confirmed that ZO1 protein levels were seemingly higher in the HRS group (Fig. 4D). The results suggested that the disruptions to ZO1 and Cx43 were alleviated by HRS treatment.

MMPs are classically known as matrix-degrading and barrier-regulating enzymes that are involved in many physiological and pathological processes (22,23). Previous studies have shown that MMP-2 and MMP-9 are important proteins that can degrade ZO1 and Cx43 (24,25). MMP activity has also been reported to be regulated by oxidative stress and inflammation (20,26). The results of the gelatin gel zymography showed that MMP-2 and MMP-9 activity in the liver decreased markedly in response to treatment with HRS (Fig. 4E). Given that MMPs can be influenced by oxidative stress (23), this result suggested another possible mechanism for AOC-induced GJ and TJ disruption, in addition to the observed changes in transcription and translation.

HRS accelerates the reversal of AOC-induced liver dysfunction in rats. The role of H_2 as a potential treatment for AOC-induced liver dysfunction was further evaluated. Timely drainage and relief of obstruction are the key treatments for patients with AOC (5). Thus, the catheter sealing caps were removed and bile was allowed to flow out 12 h after LPS infusion into the bile duct. Moreover, the animals in the various groups were subsequently treated with HRS or NS intraperitoneally, and their hepatic function was evaluated. The results showed that HRS, especially at a higher dose, potentially accelerated the reversal of AOC-induced liver dysfunction (Table III). Moreover, survival statistics also indicated that more AOC model rats survived following treatment with HRS (Fig. 4F).

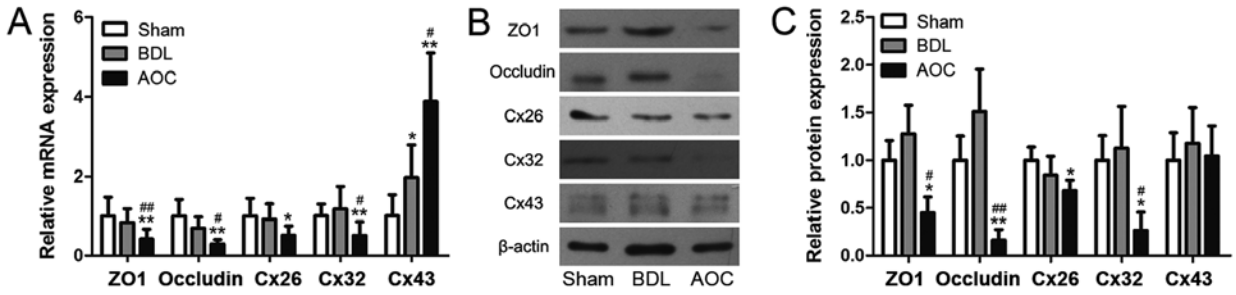

Figure 1. AOC induces disruptions in hepatocyte GJs and TJs. (A) Reverse transcription-quantitative PCR was performed to examine the expression of GJ and TJ genes in liver tissues from Sham, BDL and AOC rat models. The results demonstrated that AOC affected the expression level of junction genes. (B) Western blot and (C) densitometry analyses were performed to examine the protein levels of GJ and TJ proteins in the same liver tissues from the rat models, further corroborating the results for mRNA expression. *P<0.05 and **P<0.01 vs. sham group; $^{\#}$P<0.05 and $^{\#\#}$P<0.01 vs. BDL group. AOC, acute obstructive cholangitis; BDL, bile duct ligation; ZO1, tight junction protein 1; Cx26, gap junction protein β2; Cx32, gap junction protein β1; Cx43, gap junction protein α1; GJ, gap junction; TJ, tight junction.

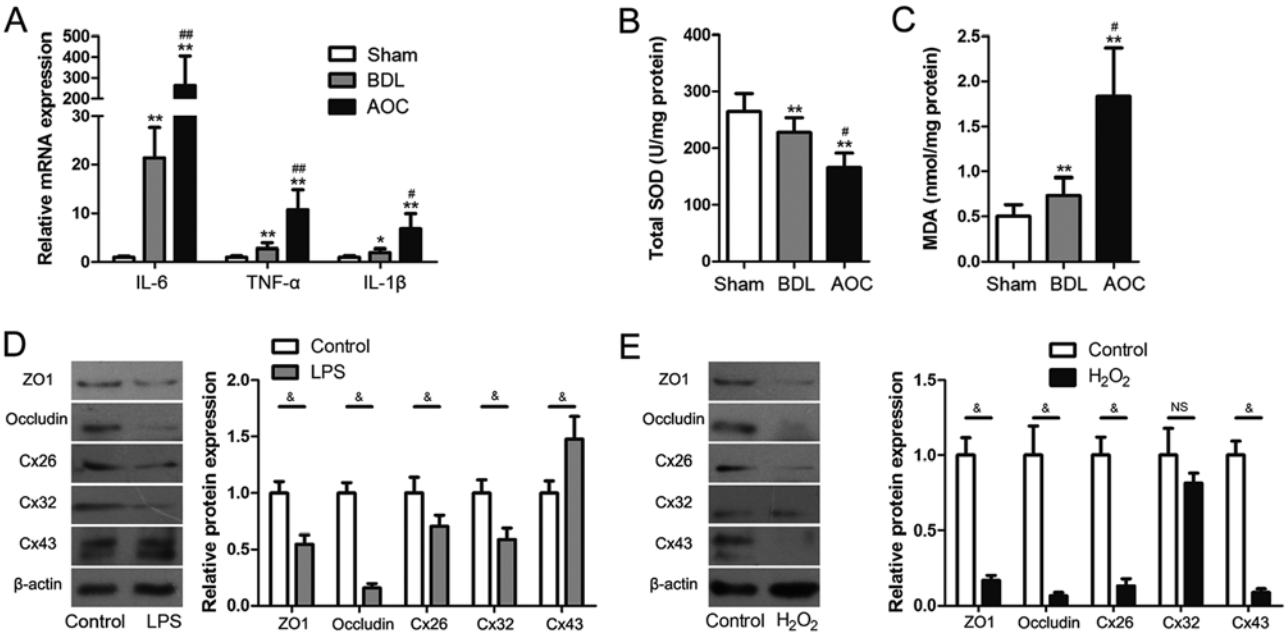

Figure 2. Inflammatory and oxidative damage arises during AOC. (A) Reverse transcription-quantitative PCR was performed to examine the expression of pro-inflammatory cytokines in liver tissues from different rat models, demonstrating that these were increased in the BDL and AOC groups compared with the Sham-operated group. (B) SOD levels decreased, while (C) MDA levels increased in liver tissues from animals in the BDL and AOC groups compared with the sham-operated group. (D) Western blotting was performed to examine the expression level of gap and tight junction proteins in BRL cells with or without LPS treatment. The protein levels following LPS treatment were similar to those observed *in vivo*. (E) Western blotting was performed to examine the expression level of gap and tight junction proteins in BRL cells with or without H_2O_2 treatment. The levels of all examined proteins, with the exception of Cx32, were reduced following H_2O_2 treatment. *P<0.05 and **P<0.01 vs. sham group; $^{\#}$P<0.05 and $^{\#\#}$P<0.01 vs. BDL group; $^{\&}$P<0.05. AOC, acute obstructive cholangitis; BDL, bile duct ligation; IL, interleukin; TNF-α, tumor necrosis factor-α; SOD, superoxide dismutase; MAD, malondialdehyde; ZO1, tight junction protein 1; Cx26, gap junction protein β2; Cx32, gap junction protein β1; Cx43, gap junction protein α1; LPS, lipopolysaccharide; NS, non-significant.

Discussion

The blood-biliary barrier is essential to maintain liver function (1). As functional components of the blood-biliary barrier, both TJs and GJs have been reported to be disrupted by cholestasis (1,27). AOC occurs as a result of biliary obstruction, which causes a rapid decrease in liver function and increases liver damage (5). Thus, it was speculated that AOC-induced liver injury may be associated with disrupted TJs and GJs. Unexpectedly, the present results indicated that TJs and GJs did not change significantly after BDL, as shown in previous studies (1,27). An acute biliary obstruction animal model was used in the present experiments, while animal models with

Table III. Liver function test results used to evaluate the degree of liver injury with or without HRS administration in AOC model rats.

	NS	HRS (5 ml/kg)	HRS (10 ml/kg)
ALT, IU/l	229.75±44.79	161.38±26.56[a]	151.14±37.39[a]
AST, IU/l	341.75±43.97	251.63±52.53[a]	261.86±45.95[a]
TBIL, μmol/l	33.83±5.33	24.43±8.18	21.19±5.46

[a]P<0.05 vs. NS group. ALT, alanine aminotransferase; AST, aspartate aminotransferase; TBIL, total bilirubin; NS, normal saline; HRS, hydrogen-rich saline.

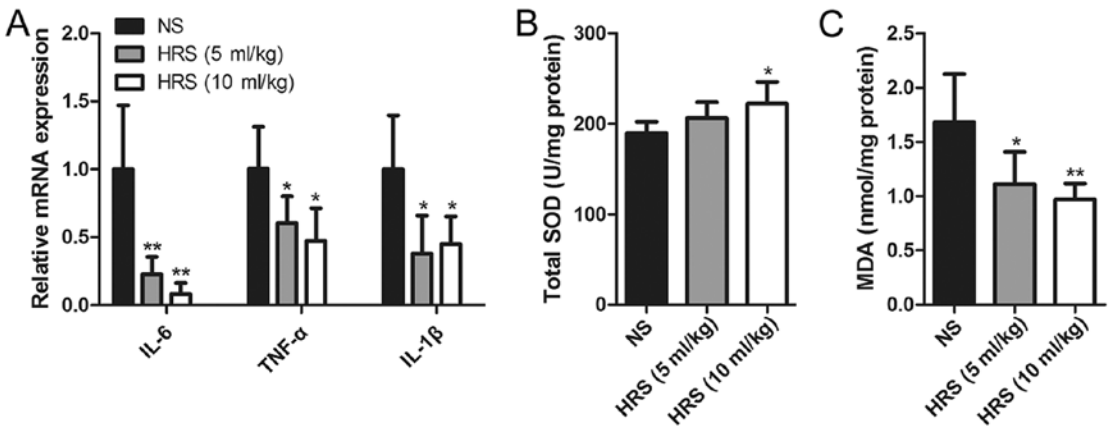

Figure 3. Molecular hydrogen attenuates AOC-induced inflammatory and oxidative damage. (A) The mRNA levels of pro-inflammatory cytokines were examined to evaluate the potential inflammatory damage with or without HRS treatment in AOC model rats. Overall, HRS treatment reduced the levels of pro-inflammatory cytokines. (B) SOD levels increased and (C) MDA levels decreased in HRS-treated animals relative to NS-treated ones, indicating that HRS treatment may have attenuated liver damage. *P<0.05 and **P<0.01 vs. respective NS group. AOC, acute obstructive cholangitis; HRS, hydrogen-rich saline; NS, normal saline; IL, interleukin; TNF-α, tumor necrosis factor-α; SOD, superoxide dismutase; MAD, malondialdehyde.

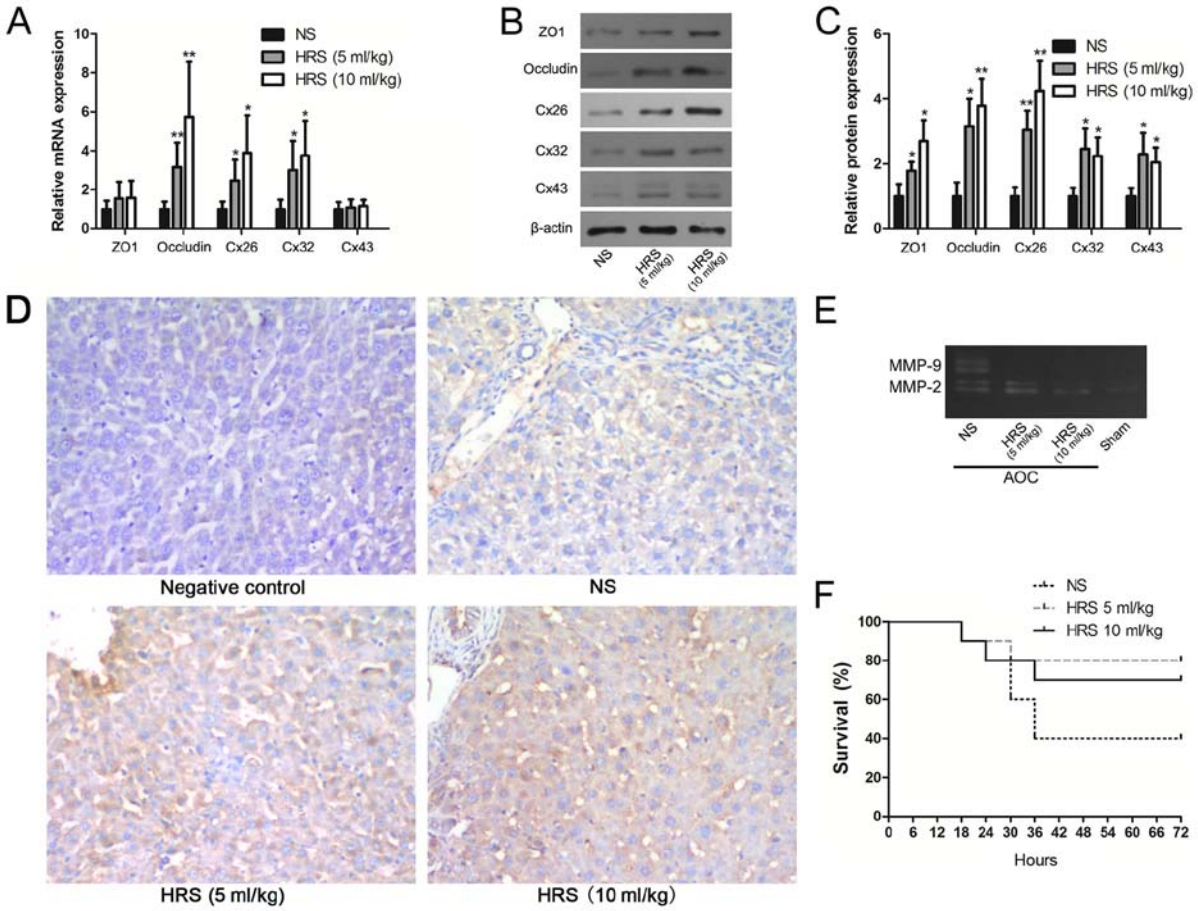

Figure 4. Molecular hydrogen reverses the AOC-induced disruption of GJs and TJs. (A) Reverse transcription-quantitative PCR, (B) western blotting and (C) respective densitometry analysis were performed to evaluate the expression of GJ and TJ proteins with or without HRS treatment in AOC model rats. (D) Immunohistochemical staining of ZO1 (counterstained with hematoxylin) in liver tissues from AOC model animals treated with NS or different doses of HRS, and from a control animal (magnification, x200). (E) Gelatin zymography demonstrating the downregulation of MMP-2 and MMP-9 activity following the administration of HRS in AOC rats compared with NS-treated ones. (F) Survival rates of AOC animals that received biliary drainage and were subsequently treated with HRS or NS, showing that HRS treatment increased the survival rates of AOC animals. *P<0.05 and **P<0.01 vs. respective NS group. AOC, acute obstructive cholangitis; HRS, hydrogen-rich saline; NS, normal saline; ZO1, tight junction protein 1; Cx26, gap junction protein β2; Cx32, gap junction protein β1; Cx43, gap junction protein α1; MMP, matrix metalloproteinase; GJ, gap junction; TJ, tight junction.

chronic biliary obstruction were used in previous studies. However, AOC induced in rats via LPS infusion following BDL caused a notable change in TJ and GJ mRNA and protein expression levels. Compared with simple biliary obstruction

models, compound injury is simultaneously induced by cholestasis and LPS, which is the most noteworthy characteristic of AOC (5). The above results revealed that abnormally expressed TJ and GJ proteins may have promoted the disruption of the blood-biliary barrier and worsened AOC-induced liver injury.

Reducing excessive inflammatory and oxidative damage may be an effective approach to accelerate the reversal of AOC-induced liver dysfunction. Due to its anti-oxidative and anti-inflammatory properties, H_2 has been reported to protect various organs, such as the heart, lung, intestine and brain, from injury (11,28-30). For hepatic diseases, H_2 has also been found to have a protective role in a variety of injuries, such as ischemia-reperfusion damage, drug-induced liver injury and hepatitis (7,31). Although studies have revealed that H_2 may also protect liver tissues from obstructive jaundice and sepsis (32,33), its role in AOC, a more rapidly progressing liver injury, remains elusive. The present results showed that hydrogen effectively accelerated the reversal of AOC-induced liver dysfunction in rats. Previous studies revealed that H_2 attenuated postoperative liver failure and accelerated liver regeneration after hepatectomy (34,35). Therefore, it is possible that molecular hydrogen may have not only a protective but also a restorative role in liver injury. However, the chemical instability of H_2 is still the main limitation of its clinical application (6). Hydrogen poses no risk of explosion in air when present at concentrations <4.6% by volume, and hydrogen inhalation at 2% has been used in previous studies (36-38). Due to the advantages in controlling the dose and route of administration, administration of hydrogen using an injectable hydrogen-rich vehicle may be a more suitable choice for specific target organs, including the liver, brain and pancreas (6). Future studies may provide a more convenient and safer delivery method of hydrogen application.

Both inflammatory and oxidative damage are common during various liver injuries (39,40). GJ protein expression is closely associated with inflammatory and oxidative damage (2,41,42). However, the relationship between TJ proteins and inflammatory or oxidative damage during liver injury remained unclear. The present results confirmed that both inflammatory and oxidative damage induced aberrant TJ and GJ protein expression in hepatocytes *in vitro*. It also provided a possible mechanism underlying the H_2-mediated rescue of GJ and TJ protein expression, due to its reported anti-oxidant and anti-inflammatory properties. Moreover, as MMPs are important regulatory enzymes that may affect both GJ and TJ proteins (24,25), their activity levels were evaluated. A number of studies have verified that junction proteins, such as occludin, ZO1, Cx32 and Cx43, are substrates of MMP-2/9 (24,43-46). Additionally, MMPs have been reported to be activated by oxidative damage, mediating junction protein cleavage (25,45). The present results showed that HRS treatment may have attenuated AOC-induced inflammatory and oxidative damage, and significantly reduced MMP-2/9 activity. This suggests that the antioxidant and anti-inflammatory properties of H_2 may reverse the disruption of junction proteins by decreasing MMP activity.

In conclusion, the present results indicated that H_2 may have accelerated the reversal of AOC-induced liver dysfunction, and this phenomenon may depend on the reversal of inhibition of GJ and TJ protein expression.

Acknowledgements

Not applicable.

Funding

This research was supported by the Zhejiang Provincial Natural Science Foundation of China (grants nos. LY17H030001 and LQ14H160001), the National Natural Science Foundation of China (grant no. 81602044), Zheng Shu Medical Elite Scholarship Fund, the Zhejiang Provincial Public Welfare Technology Application Research Projects (grants nos. 2013C33214, 2015C33293 and LGF18H030008) and the Research Foundation of Health Bureau of Zhejiang Province (grants nos. 2018238887 and 2018RC077).

Availability of data and materials

The datasets used and/or analyzed during the current study are available from the corresponding author on reasonable request.

Authors' contributions

BL designed the present study. ZZ, JY and HT performed the experiments. WL and WZ analyzed the data. JY, WZ and BL drafted and revised the paper. BL, JY, WZ and ZZ provided funding for this study. All authors reviewed the manuscript.

Ethics approval and consent to participate

This study was approved by the Ethics Committee of Zhejiang University (Hangzhou, China).

Patient consent for publication

Not applicable.

Competing interests

The authors declare that they have no competing interests.

References

1. Kojima T, Yamamoto T, Murata M, Chiba H, Kokai Y and Sawada N: Regulation of the blood-biliary barrier: Interaction between gap and tight junctions in hepatocytes. Med Electron Microsc 36: 157-164, 2003.
2. González HE, Eugenín EA, Garcés G, Solís N, Pizarro M, Accatino L and Sáez JC: Regulation of hepatic connexins in cholestasis: Possible involvement of Kupffer cells and inflammatory mediators. Am J Physiol Gastrointest Liver Physiol 282: G991-G1001, 2002.
3. Zhang Y, Sun K, Liu YY, Zhang YP, Hu BH, Chang X, Yan L, Pan CS, Li Q, Fan JY, *et al*: Ginsenoside Rb1 ameliorates lipopolysaccharide-induced albumin leakage from rat mesenteric venules by intervening in both trans- and paracellular pathway. Am J Physiol Gastrointest Liver Physiol 306: G289-G300, 2014.

4. Zhang X, Wang T, Gui P, Yao C, Sun W, Wang L, Wang H, Xie W, Yao S, Lin Y and Wu Q: Resolvin D1 reverts lipopolysaccharide-induced TJ proteins disruption and the increase of cellular permeability by regulating IκBα signaling in human vascular endothelial cells. Oxid Med Cell Longev 2013: 185715, 2013.
5. Mosler P: Diagnosis and management of acute cholangitis. Curr Gastroenterol Rep 13: 166-172, 2011.
6. Huang CS, Kawamura T, Toyoda Y and Nakao A: Recent advances in hydrogen research as a therapeutic medical gas. Free Radic Res 44: 971-982, 2010.
7. Fukuda K, Asoh S, Ishikawa M, Yamamoto Y, Ohsawa I and Ohta S: Inhalation of hydrogen gas suppresses hepatic injury caused by ischemia/reperfusion through reducing oxidative stress. Biochem Biophys Res Commun 361: 670-674, 2007.
8. Sun H, Chen L, Zhou W, Hu L, Li L, Tu Q, Chang Y, Liu Q, Sun X, Wu M and Wang H: The protective role of hydrogen-rich saline in experimental liver injury in mice. J Hepatol 54: 471-480, 2011.
9. Xie K, Liu L, Yu Y and Wang G: Hydrogen gas presents a promising therapeutic strategy for sepsis. Biomed Res Int 2014: 807635, 2014.
10. Liu W, Shan LP, Dong XS, Liu XW, Ma T and Liu Z: Combined early fluid resuscitation and hydrogen inhalation attenuates lung and intestine injury. World J Gastroenterol 19: 492-502, 2013.
11. Xie K, Yu Y, Huang Y, Zheng L, Li J, Chen H, Han H, Hou L, Gong G and Wang G: Molecular hydrogen ameliorates lipopolysaccharide-induced acute lung injury in mice through reducing inflammation and apoptosis. Shock 37: 548-555, 2012.
12. Yang J and Lu B: Establishment of a novel rat model of severe acute cholangitis. Iran J Basic Med Sci 18: 1124-1129, 2015.
13. Guidelines for the welfare of animals in rodent protection tests. A report from the rodent protection test working party. Lab Anim 28: 13-18, 1994.
14. Soothill JS, Morton DB and Ahmad A: The HID50 (hypothermia-inducing dose 50): An alternative to the LD50 for measurement of bacterial virulence. Int J Exp Pathol 73: 95-98, 1992.
15. Ohsawa I, Nishimaki K, Yamagata K, Ishikawa M and Ohta S: Consumption of hydrogen water prevents atherosclerosis in apolipoprotein E knockout mice. Biochem Biophys Res Commun 377: 1195-1198, 2008.
16. Yu P, Wang Z, Sun X, Chen X, Zeng S, Chen L and Li S: Hydrogen-rich medium protects human skin fibroblasts from high glucose or mannitol induced oxidative damage. Biochem Biophys Res Commun 409: 350-355, 2011.
17. Ohsawa I, Ishikawa M, Takahashi K, Watanabe M, Nishimaki K, Yamagata K, Katsura K, Katayama Y, Asoh S and Ohta S: Hydrogen acts as a therapeutic antioxidant by selectively reducing cytotoxic oxygen radicals. Nat Med 13: 688-694, 2007.
18. Livak KJ and Schmittgen TD: Analysis of relative gene expression data using real-time quantitative PCR and the 2(-Delta Delta C(T)) method. Method 25: 402-408, 2001.
19. Yu J, Zhang W, Qian H, Tang H, Lin W and Lu B: SOCS1 regulates hepatic regenerative response and provides prognostic makers for acute obstructive cholangitis. Sci Rep 7: 9482, 2017.
20. Cannistrà M, Ruggiero M, Zullo A, Gallelli G, Serafini S, Maria M, Naso A, Grande R, Serra R and Nardo B: Hepatic ischemia reperfusion injury: A systematic review of literature and the role of current drugs and biomarkers. Int J Surg 33 (Suppl 1): S57-S70, 2016.
21. de Andrade KQ, Moura FA, dos Santos JM, de Araújo OR, de Farias Santos JC and Goulart MO: Oxidative stress and inflammation in hepatic diseases: Therapeutic possibilities of N-acetylcysteine. Int J Mol Sci 16: 30269-30308, 2015.
22. Rodrigues SF and Granger DN: Blood cells and endothelial barrier function. Tissue Barriers 3: e978720, 2015.
23. Rosenberg GA and Yang Y: Vasogenic edema due to tight junction disruption by matrix metalloproteinases in cerebral ischemia. Neurosurg Focus 22: E4, 2007.
24. Wu J, Han W, Chen X, Guo W, Liu K, Wang R, Zhang J and Sai N: Matrix metalloproteinase-2 and -9 contribute to functional integrity and noise-induced damage to the blood-labyrinth-barrier. Mol Med Rep 16: 1731-1738, 2017.
25. Barteková M, Šimončíková P, Fogarassyová M, Ivanová M, Okruhlicová Ľ, Tribulová N, Dovinová I and Barančík M: Quercetin improves postischemic recovery of heart function in doxorubicin-treated rats and prevents doxorubicin-induced matrix metalloproteinase-2 activation and apoptosis induction. Int J Mol Sci 16: 8168-8185, 2015.
26. Amin M, Pushpakumar S, Muradashvili N, Kundu S, Tyagi SC and Sen U: Regulation and involvement of matrix metalloproteinases in vascular diseases. Front Biosci (Landmark Ed) 21: 89-118, 2016.
27. Balasubramaniyan V, Dhar DK, Warner AE, Vivien Li WY, Amiri AF, Bright B, Mookerjee RP, Davies NA, Becker DL and Jalan R: Importance of connexin-43 based gap junction in cirrhosis and acute-on-chronic liver failure. J Hepatol 58: 1194-1200, 2013.
28. Tao B, Liu L, Wang N, Tong D, Wang W and Zhang J: Hydrogen-rich saline attenuates lipopolysaccharide-induced heart dysfunction by restoring fatty acid oxidation in rats by mitigating C-Jun N-terminal kinase activation. Shock 44: 593-600, 2015.
29. Zheng X, Mao Y, Cai J, Li Y, Liu W, Sun P, Zhang JH, Sun X and Yuan H: Hydrogen-rich saline protects against intestinal ischemia/reperfusion injury in rats. Free Radic Res 43: 478-484, 2009.
30. Bai X, Liu S, Yuan L, Xie Y, Li T, Wang L, Wang X, Zhang T, Qin S, Song G, *et al*: Hydrogen-rich saline mediates neuroprotection through the regulation of endoplasmic reticulum stress and autophagy under hypoxia-ischemia neonatal brain injury in mice. Brain Res 1646: 410-417, 2016.
31. Kajiya M, Sato K, Silva MJ, Ouhara K, Do PM, Shanmugam KT and Kawai T: Hydrogen from intestinal bacteria is protective for Concanavalin A-induced hepatitis. Biochem Biophys Res Commun 386: 316-321, 2009.
32. Liu Q, Shen WF, Sun HY, Fan DF, Nakao A, Cai JM, Yan G, Zhou WP, Shen RX, Yang JM and Sun XJ: Hydrogen-rich saline protects against liver injury in rats with obstructive jaundice. Liver Int 30: 958-968, 2010.
33. Iketani M, Ohshiro J, Urushibara T, Takahashi M, Arai T, Kawaguchi H and Ohsawa I: Preadministration of hydrogen-rich water protects against lipopolysaccharide-induced sepsis and attenuates liver injury. Shock 48: 85-93, 2017.
34. Tan YC, Xie F, Zhang HL, Zhu YL, Chen K, Tan HM, Hu BS, Yang JM and Tan JW: Hydrogen-rich saline attenuates postoperative liver failure after major hepatectomy in rats. Clin Res Hepatol Gastroenterol 38: 337-345, 2014.
35. Yu J, Zhang W, Zhang R, Ruan X, Ren P and Lu B: Lactulose accelerates liver regeneration in rats by inducing hydrogen. J Surg Res 195: 128-135, 2015.
36. Cai J, Kang Z, Liu WW, Luo X, Qiang S, Zhang JH, Ohta S, Sun X, Xu W, Tao H and Li R: Hydrogen therapy reduces apoptosis in neonatal hypoxia-ischemia rat model. Neurosci Lett 441: 167-172, 2008.
37. Matchett GA, Fathali N, Hasegawa Y, Jadhav V, Ostrowski RP, Martin RD, Dorotta IR, Sun X and Zhang JH: Hydrogen gas is ineffective in moderate and severe neonatal hypoxia-ischemia rat models. Brain Res 1259: 90-97, 2009.
38. Hayashida K, Sano M, Ohsawa I, Shinmura K, Tamaki K, Kimura K, Endo J, Katayama T, Kawamura A, Kohsaka S, *et al*: Inhalation of hydrogen gas reduces infarct size in the rat model of myocardial ischemia-reperfusion injury. Biochem Biophys Res Commun 373: 30-35, 2008.
39. Li S, Tan HY, Wang N, Zhang ZJ, Lao L, Wong CW and Feng Y: The role of oxidative stress and antioxidants in liver diseases. Int J Mol Sci 16: 26087-26124, 2015.
40. Gao B: Hepatoprotective and anti-inflammatory cytokines in alcoholic liver disease. J Gastroenterol Hepatol 27 (Suppl 2): 89-93, 2012.
41. Santolim LV, Amaral MECD, Fachi JL, Mendes MF and Oliveira CA: Vitamin E and caloric restriction promote hepatic homeostasis through expression of connexin 26, N-cad, E-cad and cholesterol metabolism genes. J Nutr Biochem 39: S86-S92, 2017.
42. Gagliano N, Donne ID, Torri C, Migliori M, Grizzi F, Milzani A, Filippi C, Annoni G, Colombo P, Costa F, *et al*: Early cytotoxic effects of ochratoxin A in rat liver: A morphological, biochemical and molecular study. Toxicology 225: 214-224, 2006.
43. Chaturvedi M and Kaczmarek L: Mmp-9 inhibition: A therapeutic strategy in ischemic stroke. Mol Neurobiol 49: 563-573, 2014.
44. Ren C, Li N, Wang B, Yang Y, Gao J, Li S, Ding Y, Jin K and Ji X: Limb ischemic perconditioning attenuates blood-brain barrier disruption by inhibiting activity of MMP-9 and occludin degradation after focal cerebral ischemia. Aging Dis 6: 406-417, 2015.
45. Bauer AT, Bürgers HF, Rabie T and Marti HH: Matrix metalloproteinase-9 mediates hypoxia-induced vascular leakage in the brain via tight junction rearrangement. J Cereb Blood Flow Metab 30: 837-848, 2010.
46. Lischper M, Beuck S, Thanabalasundaram G, Pieper C and Galla HJ: Metalloproteinase mediated occludin cleavage in the cerebral microcapillary endothelium under pathological conditions. Brain Res 1326: 114-127, 2010.